0026-895X/03/6303-499–511$7.00
MOLECULAR PHARMACOLOGY
Copyright © 2003 The American Society for Pharmacology and Experimental Therapeutics
Mol Pharmacol 63:499–511, 2003

Vol. 63, No. 3
1953/1043806
Printed in U.S.A.

Molecular Modeling of Interactions of Dihydropyridines and Phenylalkylamines with the Inner Pore of the L-Type Ca^{2+} Channel

GREGORY M. LIPKIND and HARRY A. FOZZARD

Cardiac Electrophysiology Labs, Departments of Biochemistry & Molecular Biology and Medicine, the University of Chicago, Chicago, Illinois

Received June 26, 2002; accepted November 7, 2002

This article is available online at http://molpharm.aspetjournals.org

ABSTRACT

Domains IIIS5, IIIS6, and IVS6 transmembrane segments of L-type Ca^{2+} channels participate in dihydropyridine (DHP) and phenylalkylamine (PAA) binding. The inner pore structure of the $Ca_v1.2$ channel was reconstructed from coordinates of the transmembrane α-helices of the KcsA channel. S6s were aligned with M2 by comparative analysis of the pore-facing M2 side chains and those required for drug binding. Two neighboring tilted S6 helices of domains III and IV below the selectivity filter formed an interdomain crevice. Docking of DHPs inside this crevice located the DHP ring between Phe-1159 of IIIS6 and Ala-1467 of IVS6, parallel to the pore axis, whereas the 4-aryl ring participated in aromatic and polar interactions with the side chains of Tyr-1152 and Tyr-1463. Nonpolar interactions of the port side ester group with hydrophobic side chains of Ile-1156, Ile-1163, and Ile-1471 on the bottom of the binding cavity, formed by the crossover of IIIS6 and IVS6, could stabilize the channel's closed/inactivated state. Similar arrangements were found for DHP agonist drugs, except for the absence of hydrophobic interactions with the helical crossing. In this arrangement, DHPs do not physically block the pore. Locating the central amine group of desmethoxyverapamil near the selectivity filter domain III glutamic acid allows one aromatic ring through its CH_2CH_2 linker to interact with the side chain of Tyr-1463 inside the DHP binding site, whereas the opposite aromatic ring is in contact with the side chain of Ile-1470 of IVS6, blocking the pore.

Voltage-gated Ca^{2+} channels are important pharmacological targets for treatment of cardiovascular disease (Triggle, 1999). Commonly used drugs fall into three distinct classes: phenylalkylamines (PAA), benz(othi)azepines (BTZ), and dihydropyridines (DHP) (Hockerman et al., 1997b; Mitterdorfer et al., 1998). Among the most potent are the 1,4 DHPs, including derivatives inhibiting Ca^{2+} current (antagonists) and derivatives increasing Ca^{2+} current (agonists). Each drug type has separate but overlapping, or allosterically linked, binding sites in Ca^{2+} channels. Many residues important for binding of Ca^{2+} channel antagonists have been identified, and substantial progress has been made in characterizing the Ca^{2+} channel pore structure. If available pore models are accurate, then they should predict a drug binding region that can be experimentally tested.

Voltage-gated Ca^{2+} channels belong to a structurally homologous superfamily of voltage-gated channels, including K^+ and Na^+ channels (Hille, 2001), with four homologous domains or subunits of six transmembrane segments S1 to S6, arranged symmetrically around a central pore. The selectivity filter is formed by parts of the four S5–S6 extracellular segments (P loops). The outer pore is lined by these P loops and the inner pore is lined by four S6 segments and possibly four S5 segments. X-ray crystallographic analysis of the pore-forming portions of the bacterial K^+ channels KcsA and MthK (Doyle et al., 1998; Jiang et al., 2002a) has confirmed previous assumptions about structural topology of voltage-gated channels. The KcsA channel has four subunits, each with two transmembrane segments, M1 and M2, forming an "inverted teepee". P loops formed from the K^+ channel M1–M2 connecting segment compose the 3-Å diameter selectivity region, which is lined by main chain carbonyls of the TVGYG "signature sequence". The Ca^{2+} channel selectivity region must be different, because P loop side chains play crucial roles in determining the channel selectivity. Ca^{2+} channel P loops contain a highly conserved pattern of four glutamates (the EEEE locus), forming the selectivity region (Heinemann et al., 1992; Yang et al., 1993; Stea et al., 1994).

In our Ca^{2+} channel outer vestibule model (Lipkind and Fozzard, 2001), we used the crystal structure of the KcsA

Supported by United States Public Health Service grant R01-HL65661.

ABBREVIATIONS: DHP, dihydropyridine; PAA, phenylalkylamine; BTZ, benzothiazepine; PN 200-110, (+)-isradipine; D888, desverapamil; $Ca_v1.2$, the L-type Ca^{2+} channel; IIIS5 and S6, domain III 5th and 6th transmembrane segments; IVS6, domain IV 6th transmembrane segment; KcsA, K^+ channel from *Streptomyces lividans*; MthK, K^+ channel from *Methanobacterium thermoautotrophicum;* M1 and M2, the two transmembrane segments of the bacterial channel subunits.

channel, with adaptation of the P loops and the selectivity filter to accommodate the roles of side chains in the selectivity process. This procedure located the glutamate selectivity ring at the level of Met-96 of the KcsA M2 helices. It is likely that the KcsA structure is of a closed channel (Jiang et al., 2002b). A major feature of drug binding to the L-type Ca^{2+} channel is the dramatic increase in drug affinity upon activation/depolarization. The structure of an open Ca^{2+}-activated K^+ channel (MthK) is almost identical, but it shows a hinged bend in the M2 helix (Jiang et al., 2002a). However, the critical glycine residues forming the hinge are missing from the L-type Ca^{2+} channel domains III and IV S6 helices, so that modeling of the Ca^{2+} channel's open state is not feasible at this time.

Binding sites for all three classes of drugs are located below the channel's selectivity filter. Indeed, quaternary amine derivatives of PAA (verapamil) gain access to their binding site from the cytoplasm (Hockerman et al., 1997b) and seem to inhibit the central pore by physical occupancy. PAAs block the binding of both DHPs and BTZs, reflecting the likely proximity of their individual binding sites (Hockerman et al., 1997b; Mitterdorfer et al., 1998). Experiments with block by derivatives of amlodipine, where the outer group of the DHP ring was connected through alkyl spacers to a permanently charged head group, have also located the DHP binding site deep inside the channel, about 14 Å from the extracellular surface (Bangalore et al., 1994).

For reconstruction of the DHP and PAA binding sites, we followed the methodology that we used for modeling the outer vestibule of the Ca^{2+} channel, populating the KcsA M1 and M2 backbones with side chains of the respective L-type Ca^{2+} channel S5 and S6 amino acid sequences (Lipkind and Fozzard, 2001). The interface between the S6 α-helices of domains III and IV, restricted above by P loop and selectivity filter residues, can form a binding site outside of the central pore for both antagonists and agonists of the DHP family. Critical hydrophobic interactions of the antagonist port side ester group with the helical IIIS6/IVS6 crossover residues stabilize channel closure, and these interactions are absent for agonists. PAAs in this site partially occlude both the DHP binding site and the central pore and block Ca^{2+} channels by direct interaction with the selectivity filter glutamates.

Materials and Methods

Modeling was accomplished in the Insight and Discover graphical environment (MSI, Inc., San Diego, CA), as described previously (Lipkind and Fozzard, 2000, 2001). Molecular mechanics energetic calculations used the consistent valence force field approximation. For minimization procedures, the steepest descents and conjugate gradients were used.

Results and Discussion

Residues Identified as Important for Drug Binding. Different experimental approaches (photoaffinity labeling, construction of chimeric channels between L-type and non–L-type Ca^{2+} channels) suggest that the two S6 transmembrane segments of domains III and IV interact with the antagonists (Hockerman et al., 1997b; Mitterdorfer et al., 1998). In addition, the intermediate part of the domain III S5 also contributes to antagonist binding (Grabner et al., 1996). Alanine-scanning mutagenesis has identified specific amino acid residues that interact directly with each class of drugs. The data from alanine-scanning mutagenesis of III S6 and IV S6 of $Ca_v1.2$ for binding of (+)-[^{3}H]isradipine (PN 200-110) (Peterson et al., 1996, 1997) are presented in Table 1. Ten amino acid residues were identified whose mutations reduced the affinity for PN 200-110 by 2- to 25-fold. Four amino acid residues of the domain IV S6—Tyr-1463, Met-1464, Ile-1471, and Asn-1472—have been found to be crucial for binding of DHPs. Using a similar approach, Schuster et al. (1996) distinguished only three domain IV S6 amino acids—Tyr-1463, Met-1464, and Ile-1471; simultaneous mutation of these three residues reduced isradipine affinity by >100-fold. The largest effects of mutations in IIIS6 were seen in positions Tyr-1152, Ile-1153, Ile-1156, Phe-1159, and Met-1161, with affinity decrease of 5- to 25-fold (Table 1), where Tyr-1152 and Phe-1159 are conserved between DHP-sensitive and -resistant isoforms (Peterson et al., 1997). It is remarkable that the mutant Y1152F has a K_d value 12.4-fold higher than that of the wild-type channel, so the phenolic hydroxyl group of Tyr-1152 must also be important for DHP binding (Peterson et al., 1996). These data also indicate the very local character of DHP binding to only three successive turns of both IIIS6 and IVS6. Moreover, the amino acid residues of IIIS6 and IVS6 that are required for binding of isradipine are located in nearly analogous positions in the putative α-helices. This suggests a domain interface model of DHP binding, with the drugs located between two inner faces of the IIIS6 and IVS6 segments (Hockerman et al., 1997b).

The PAA binding pocket is composed of at least seven amino acid residues (Table 2; Hockerman et al., 1995, 1997a), based on the alanine scanning mutagenesis of binding of the PAA derivative desmethoxyverapamil (D888). Three amino acid residues in segment IVS6—Tyr-1463, Ala-1467, and Ile-1470—are required for high-affinity block by D888, because their mutation reduced affinity 6- to 12-fold (Table 2). The same conclusion was reached by Schuster et al. (1996). However, Hering et al. (1996) also included Met-1464 as a residue contributing to high-affinity PAA interaction. Four amino acid residues of IIIS6 that are entirely conserved throughout L-type and non–L-type Ca^{2+} channels can participate in PAA

TABLE 1
Effects of alanine mutations in domains III and IV S6 segments of the L-type Ca^{2+} channel on binding of isradipine ((+)-[^{3}H]PN200–110)

IIIS6 Mutation	Mutant IC_{50}/Native IC_{50}	IVS6 Mutation	Mutant IC_{50} /Native IC_{50}
Y1152A	25	Y1463A	2.9
(Y1152F)	12.4	M1464A	1.6
I1153A	6.2	I1471A	2.7
I1156A	17	N1472A	8.9
F1159A	4.5		
M1160A	3.5		
M1161A	9.6		

Data from Peterson et al. (1997).

binding—Tyr-1152, Ile-1153, Phe-1164, and Val-1165 (Hockerman et al., 1997a). However, we note some possibly contradictory results for mutations of Tyr-1152. Y1152F decreased the affinity to D888 by 19-fold, but the alanine mutation in this position increased affinity by 6.3-fold. At the same time, the two residues, Phe-1164 and Val-1165, which are very close to the intracellular C-end of IIIS6 and are uninvolved in DHP binding, showed a ~10-fold decrease in affinity for D888 upon alanine substitution.

S5 and S6 Alignment. The critical step in modeling of the inner pore of the L-type Ca^{2+} channel on the basis of the KcsA structure was to determine how the Ca^{2+} channel residues are aligned on the M1 and M2 α-helical backbones. To develop our original Ca^{2+} channel pore model (Lipkind and Fozzard, 2001), we hypothesized that the residues interacting with drugs within the pore are facing the pore. Such an arrangement maximizes the coincidence of the DHP- and PAA-sensing residues with the pore-facing residues of KcsA. The walls of the inner pore of the KcsA channel are formed by adjacent pairs of residues: Val-95 and Met-96, Gly-99 and Ile-100, Phe-103 and Gly-104, and Thr-107. Doyle et al. (1998) found that the aromatic and hydrophobic rings of the N-terminal Trp residues of M2 α-helices play an important role in arrangement of the helices within the membrane. We began our alignment of this Trp residue of KcsA with the hydrophobic Phe-1454 residue on the N-end of domain IV S6 (Stea et al., 1994). This places Tyr-1463, so important for binding both DHPs and PAAs, on the level of the pair Val-95 and Met-96. The same is true for Tyr-1152 of domain IIIS6. This alignment sets four possible assignments of all of the IIIS6 and IVS6 $Ca_v1.2$ residues (Table 3). Table 3 shows two possible alignments of the $Ca_v1.2$ IIIS6 and IVS6 segments with the KcsA M2. For discussion, the alignments will be referenced as follows: alignment 1 for both segments, 1,1; alignment 2 for both segments, 2,2; alignment 1 for IIIS6 and alignment 2 for IVS6, 1,2; alignment 2 for IIIS6 and alignment 1 for IVS6, 2,1. If Met-96 is chosen for location of the Tyr residues (alignment 1,1 of Table 3 for IIIS6 and IVS6, respectively), the locations of the Ca^{2+} channel residues are shown in Fig. 1, after energy minimization. This is the alignment we used previously for modeling of the L-type Ca^{2+} channel (Lipkind and Fozzard, 2001). The teepee structure of the S6 α-helices leads to wide separation of the helices near the extracellular side of the pore, opening a space between the pore-facing residues of IIIS6 and IVS6. That additional space permits antagonist molecules to be located in the resulting interface crevice, as well as inside the pore. For alignment 1,1, the side chains of both drug-sensitive Tyr-1152 and Tyr-1463 residues face the pore and are located close enough to interact simultaneously with DHP and PAA molecules. Phe-1159 and Ala-1467 form the opposing walls of the interface crevice. The mutation F1159A decreased binding of DHP 5-fold (Peterson et al., 1997), and substitutions of Ala-1467 decreased significantly binding of PAA (Hockerman et al., 1995). The bottom of the crevice is formed by close contacts between bulky hydrophobic residues Ile-1163 of IIIS6 and Ile-1471 of IVS6. Ile-1471 participates in the binding of isradipine (Peterson et al., 1997). The neighboring Ile-1470 is important for binding of PAA; its substitution by Ala reduces binding of D888 by 6-fold (Hockerman et al., 1997a). Therefore, on the level of these isoleucines, PAAs and DHPs interact with different sides of the same α-helix of IVS6. However, only for the alignment 1 of IVS6, when Tyr-1463 of IVS6 coincides with the location of Met-96 of M2, do the side chains of both Ile-1470 and Ile-1471 face the pore. In the alternative alignment 2 for IVS6, Tyr-1463 is at the level of Val-95 of M2, and Ile-1470, corresponding in this case to Ser-102 of KcsA, is directed outside of the pore and makes immediate contacts with the neighboring α-helix of IVS5 segment. Consequently, in this alignment, Ile-1470 is not able to interact with PAA. Another disadvantage of alignment 2 of IVS6 is that the pore-facing residue Ile-100 of M2 is substituted by Phe-1468 of IVS6, and its bulky aromatic side chain fills the space inside the crevice, preventing binding of antagonists in the interface between domains III and IV. In alignment 1 for IVS6, this position is occupied by the small residue of Ala-1467 (Table 3), which is conserved in all DHP-sensitive Ca^{2+} channels (Stea et al., 1994). Moreover, in the alternative alignment 2 of IVS6, Tyr-1463, substituting for Val-95 of M2, is located in a position removed from the interface crevice. Altogether, these considerations give preference to alignment 1 of IVS6 when its Tyr-1463 coincides with Met-96 of the KcsA M2.

Alignment 1 for domain IIIS6 directs inside the pore not only the side chain of Tyr-1152 of IIIS6 but also that of Ile-1156, which are both available for drug interaction (Fig. 1). Ile-1156 is most sensitive to interaction with DHP, because its substitution by Ala reduced isradipine binding affinity 17-fold (Peterson et al., 1997). However, the side chains of the two amino acid residues Ile-1153 and Met-1161, which show moderate affinity changes with substitution by Ala (~6- and 9-fold, Table 1), are located outside the interdomain cavity in alignment 1 of IIIS6. From this point of view, alignment 2 of IIIS6, where Tyr-1152 coincides with Val-95 of M2, seems to be preferable. This results in Tyr-1152, Ile-1153, Ile-1156, and Met-1161 facing the interface crevice between domains IIIS6 and IVS6. Therefore, a reasonable candidate for alignment is 2,1 (i.e., alignment 2 for domain IIIS6 and alignment 1 for domain IVS6). From this analysis we cannot distinguish unequivocally between alignments 1,1 and 2,1; therefore, both must be considered further.

The transmembrane segment IIIS5 may also be involved in DHP binding (Grabner et al., 1996), even though it was not photolabeled by any of the photoreactive DHPs. Mutational analysis has distinguished two amino acid residues of IIIS5

TABLE 2
Effects of alanine mutations on domains III and IV S6 segments of the L-type Ca^{2+} channel on binding of (−)-D888

IIIS6 Mutation	Mutant IC_{50}/Native IC_{50}	IVS6 Mutation	Mutant IC_{50}/Native IC_{50}
Y1152A	0.16	Y1463A	9.6
I1153A	12.8	(A1467S)	10.8
F1164A	9.5	I1470A	6.2
V1165A	9.5		

Data from Hockerman, et al. (1995; 1997a).

that contribute to DHP binding, Thr-1039 and Gln-1043 (Mitterdorfer et al., 1996; He et al., 1997). Both amino acids face the same side of an α-helix. Therefore, it was logical to align these Thr-1039 and Gln-1043 with those residues of the outer M1 α-helix of KcsA that could form the back wall of the interface crevice—Thr-32 and Leu-36 (Table 4). In this case, the conserved Gly residue in the C terminus ends of S5 segments (see Lipkind and Fozzard, 2001), Gly-1050 of IIIS5 of $Ca_v1.2$, coincides with the identical Gly-43 of KcsA. This is important, because in the KcsA structure, Gly-43 is in immediate contact with the side chain of Val-91 of M2, and substitution of this small Gly by any other amino acid except Ala would disrupt the relationship between the helices. In the position corresponding to Val-91 the IIIS6 segment contains Ile-1147 (Table 3). The huge 1000-fold decrease in affinity for isradipine by T1039Y mutant (He et al., 1997) is probably an indirect effect of substitution of Thr-1039 by the bulky Tyr residue (Wappl et al., 2001). Using KcsA as the structural template, we find that the side chain of Thr-1039 is screened by amino acid residues of the IIIS6 α-helix located closer to the pore, consistent with an indirect effect of its mutation. Gln-1043 forms part of the back wall of the cavity (Fig. 1), where it could participate in interactions with DHP or PAA (Wappl et al., 2001).

TABLE 3
Two alignments of IIIS6 and IVS6 segments of the L-type Ca^{2+} channel with M2 segments of the KcsA channel

	Alignment 1		Alignment 2	
KcsA	IIIS6	IVS6	IIIS6	IVS6
Trp-87	Val-1143	Phe-1454	Glu-1144	Ala-1455
Gly	Glu	Ala	Ile	Val
Arg	Ile	Val	Ser	Phe
Leu	Ser	Phe	Ile	Tyr
Val	Ile	Tyr	Phe	Phe
Ala	Phe	Phe	Phe	Ile
Val	Phe	Ile	Ile	Ser
Val	Ile	Ser	Ile	Phe
Val	Ile	Phe	Tyr-1152	Tyr-1463
Met-96	Tyr-1152	Tyr-1463	Ile	Met
Val	Ile	Met	Ile	Leu
Ala	Ile	Leu	Ile	Cys
Gly	Ile	Cys	Ile	Ala
Ile-100	Ile	Ala	Ala	Phe
Thr	Ala	Phe	Phe	Leu
Ser	Phe	Leu	Phe	Ile-1470
Phe-103	Phe	Ile-1470	Met	Ile-1471
Gly	Met	Ile-1471	Met	Asn
Leu	Met	Asn	Asn	Leu
Val	Asn	Leu	Ile	Phe
Thr-107	Ile	Phe	Phe	Val
Ala	Phe	Val	Val	Ala
Ala	Val	Ala	Gly	Val
Leu	Gly	Val	Phe	Ile
Ala	Phe	Ile	Val	Met
Thr	Val	Met	Ile	Asp

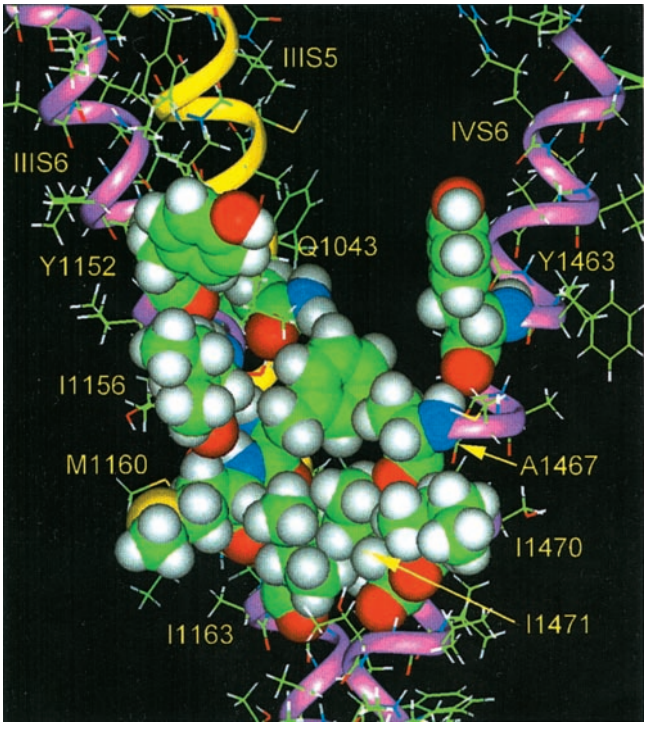

Fig. 1. Interface crevice. The modeled structure of the interface crevice between S6 α-helices of domains III and IV (shown by pink ribbons) for the alignment of Tyr-1152 and Tyr-1463 of the L-type Ca^{2+} channel with Met-96 of the M2 helix of the KcsA channel (alignment 1,1 in Table 3), with the pore-facing residues shown by space-filling images. The S5 α-helix of domain III is shown by a yellow ribbon.

Huber et al. (2000) have proposed a different alignment for the transmembrane segments of the L-type Ca^{2+} channel on the basis of sequence homology with the KcsA channel by optimizing the coincidence of identical amino acids. However, homology by this criterion is limited; there are only four identical residues between IVS6 and M2, and only one between IIIS6 and M2. In that alignment, the important residue Tyr-1152 of IIIS6 is excluded from the interface crevice entirely, and the side chains of Tyr-1152 (IIIS6) and Tyr-1463 (IVS6) are ~27 to 30 Å apart, making it impossible for simultaneous interaction of these two DHP-sensing residues with DHP molecules. Moreover, Huber et al. (2000) align Phe-1046 of IIIS5 segment with Gly-43 of KcsA M1, which is stereochemically unlikely. The wide opening of their proposed DHP binding site accommodates the DHP molecule. However, their modeled structure fails to include the essential outer vestibule P loops (see below), which would interfere with their binding cavity. The absence of P loops in the model of Zhorov et al. (2001) also restricts the reliability of their conclusions.

The Interdomain (III and IV) Antagonist Binding Site and the Selectivity Filter. Because the P loop structure must fit between the adjacent S6 segments, it is evident that antagonist binding sites inside the inner pore are restricted by the amino acid residues of the P loops and the selectivity filter. Location of the P loops in the KcsA X-ray data are not sufficient to guide their location in the Ca^{2+} channel, because the selectivity filter structures must be different. The KcsA selectivity filter is 12 Å long and formed by the four signature sequences TVGYG (75–79 in KcsA), whereas in the Ca^{2+} channel, the side chain of only one glutamic acid from each domain participates in the selectivity filter. In the KcsA structure the sequences Met-96 to

TABLE 4
Alignment of IIIS5 segment of the L-type Ca^{2+} channel with M1 of the KcsA channel

									36											
M1	A	A	G	A	A	T	V	L	L	V	I	V	L	L	A	G	S	Y	L	A	V
IIIS5	I	V	I	V	T	T	L	L	Q	F	M	F	A	C	A	G	V	Q	L	F	K
									1043											

Ile-100 (MVAGI) of the inner M2 α-helix, which were aligned with the DHP or PAA sensing residues of Ca^{2+} channels—Tyr-1152, Tyr-1463, Ile-1153, Ile-1156, and Ala-1467 (Table 3)—are screened from the pore by van der Waals contacts with the side chains of neighboring P loops (Thr-74, Thr-75). Also, it is important that Gly-99 of the M2 segment of KcsA, which is very conserved in all K^+ channels and provides immediate steric contact between the C^{α}-H bond of this residue and the main chain carbonyl of Ala-73 of the P loop (Doyle et al., 1998), be replaced by the bulky residues of Ile in Ca^{2+} channels (Table 3). Such a substitution is impossible in K^+ channels. Therefore, the selectivity filter of the Ca^{2+} channel must be located higher, closer to the extracellular side of the membrane. As we previously considered for modeling of the outer vestibules of Na^+ and Ca^{2+} channels (Lipkind and Fozzard, 2000, 2001), the narrowing walls of the S6 teepee restrict the location of the vestibule frame consisting of the four α-helix-turn-β-strand P loops approximately to the level of Ile-1575 of IVS6 of the Na^+ channel or of Tyr-1463 of IVS6 of the Ca^{2+} channel. In both cases, we align these residues with Met-96 of M2, coinciding with the data of alanine scanning mutagenesis for the $Ca_v1.2$ channel. The first residues in domains IIIS6 and IVS6 to influence binding of isradipine and D888 were Tyr-1463 of IVS6 and Tyr-1152 of IIIS6, both in the 10th position from the N terminus of the α-helix. S6 residues near the Tyr residues all had no effect on block by DHP or PAA (Hockerman et al., 1997b; Mitterdorfer et al., 1998). Presumably, dense packing by residues of the P loops or by the selectivity filter prevents access to the residues in the first nine positions in the S6 helices.

In support of the location of the P loops near Tyr-1463 of IVS6, that residue is intimately connected with the selectivity and permeation process. Its mutation to alanine alters the Ca^{2+} channel reversal potential by -15 mV (61 mV in the wild-type channel and 46 mV in the Y1463A mutant). It also increases permeation by *N*-methyl-D-glucamine (Hockerman et al., 1995), suggesting that Tyr-1463 is indeed located near the selectivity filter, perhaps contributing to its structural integrity. The same is true for Tyr-1152; its mutation to alanine also affected selectivity (Hockerman et al., 1997a). It is therefore necessary to locate the four glutamic acids of the selectivity filter (the EEEE locus), arranged for formation of the high affinity Ca^{2+} binding site, at the level of Tyr-1463 and Tyr-1152. At the same time, the P loop and selectivity filter location must also allow the aromatic rings of both of these Tyr residues to be accessible to DHP and PAA from below the selectivity ring.

Before consideration of the binding site for DHPs and PAAs inside the pore, we need to note that our reconstruction of the inner pore of Ca^{2+} channels does not coincide exactly with that of the KcsA channel. The α-helices of the Ca^{2+} channel P loops must be more distant from the pore axis than the KcsA P loop α-helices to allow room for the glutamate side chains to form the selectivity ring. Consequently, the S5 helices are slightly displaced outward relative to the M1 segments (Lipkind and Fozzard, 2001). Optimization of the potential energy of the assembly of P loops and S5 and S6 helices led also to additional minimal adjustment of the S6 helices in the outward direction (1.5–2.0 Å). Displacement of the S6 helices is also determined by the requirements of packing of side chains in the narrowest part of the teepee, which occurs at the crossing of the S6 helices. In the KcsA channel, the immediate contacts of neighboring M2 helices at this level are realized by approach of small amino acids: Thr-107 and Ala-111 from one M2 helix to Gly-104 and Ala-108 of M2 of the adjacent subunit (Doyle et al., 1998), whereas in our Ca^{2+} channel model, the corresponding positions are substituted by amino acid residues with bulky side chains—Ile, Val, and Phe (Table 3). The locations of the S6 helices were recalculated to allow optimal packing of these bulky side chains, with contacts between Ile-1163 and Phe-1167 of IIIS6 and Ile-1471, Val-1475, and Ile-1478 of IVS6.

After arrangement of the plane of the selectivity filter relative to the pore, we examined the structure of the antagonist binding site in the interdomain crevice formed by IIIS6, IIIS5, and IVS6 segments according to both of the alternative alignments 1,1 and 2,1 (Table 3). Using alignment 1,1, the binding site is shown in Fig. 2, left. On the upper level, the crevice is restricted by the side chain of Glu-1118 and the main chain of the neighboring Phe-1117 of the P loop of domain III, which are surrounded by the side chains of Tyr-1152 of IIIS6 and Tyr-1463 of IVS6. This places the side chains of the tyrosines near the top of the binding site (Fig. 2A, left), a little lower than the glutamic acids of the selectivity filter, where they are available for interaction with drugs inside the cavity. The bottom of the interdomain crevice is restricted by the side chains of bulky hydrophobic residues of Ile-1163 (IIIS6) and Ile-1471 (IVS6) at the III/IV S6 crossing. The side walls of the cavity are formed by the side chains of Phe-1159 (IIIS6) and Ala-1467 (IVS6) with separation of ~4 to 4.5 Å. The residues N-terminal to Glu-1118 of the P loop (Phe-1117, Thr-1116, and Ser-1115) and the side chains of Ile-1155, Phe-1159, and Asn-1162 of domain IIIS6 and Met-1464, Phe-1468, and Asn-1472 of domain IVS6 contribute to the back wall of this cavity. It is unlikely that the S4 voltage sensor and its surrounding water-filled compartment are behind the binding

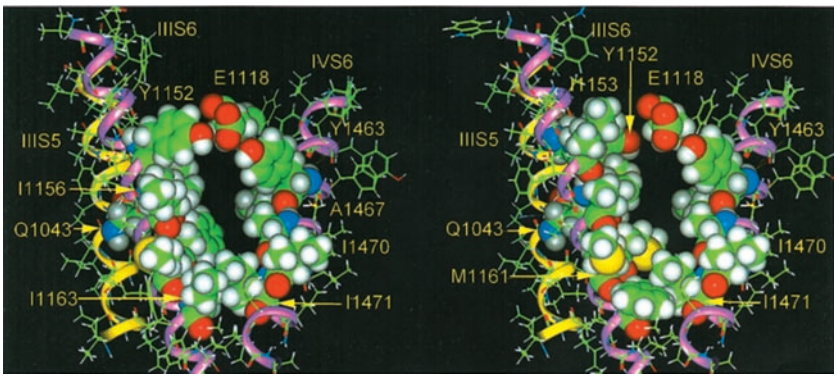

Fig. 2. Comparison of alternative alignments. The interface III/IV binding site of the L-type Ca^{2+} channel formed by S6 α-helices and restricted on the top by the side chain of residue Glu-1118 (domain IIIP) of the selectivity filter. The structure of the site in the case of alignment of Tyr-1152 of domain IIIS6 with Met-96 of KcsA and Tyr-1463 of domain IVS6 with Met-96 of KcsA (alignment 1,1 of Table 3) is shown in the left, whereas for alignment of Tyr-1152 with Val-95 and Tyr-1463 with Met-96 (alignment 2,1 of Table 3), it is shown in the right.

cavity; more likely, the cavity wall is in contact with hydrophobic regions of the protein and/or the lipid bilayer. The alternative alignment 2,1 (shifting IIIS6; Table 3) places Tyr-1152 to coincide with Val-95 of KcsA M2. It seems less acceptable because accessibility to the side chain of Tyr-1152 is restricted by the main chains of residues Phe-1117 and Glu-1118 of the P loop and the side chain of Ile-1156 of IIIS6 itself (Fig. 2, right). Therefore, the next step is to consider docking DHP and PAA into this crevice constructed with alignment 1,1 (Fig. 2, left).

Conformation of the DHP for Docking in the Binding Site. Before docking the DHP molecule, we need to consider its conformational possibilities, which have been described comprehensively by Goldmann and Stoltefuss (1991). The most characteristic representative of the DHP family is nifedipine (Fig. 3A). The DHP ring itself is nearly planar and exists in a flattened boat conformation with the 4-aryl substituent at C4 occupying the pseudoaxial position perpendicular to the plane of the DHP ring. In DHP structures, the polar group inside of the 4-aryl ring (here NO_2) is maximally distant from the NH bond at the stern of the DHP ring. If the 4-aryl ring is up, then two sides of the DHP ring can be distinguished—the port (left) side and the starboard (right) side. The ester substituents of the DHP ring could adopt various conformations. At the same time, assuming a favored coplanar arrangement of the ester carbonyl group relative to the double bond of the DHP ring, two conformations are possible for the ester groups on each side: *trans* and *cis*, where the carbonyl group is located in the *trans*- or *cis*-position relative to the DHP ring double bond. X-ray analysis shows a preference for the *cis* arrangement of the ester group on the port side, whereas the ester group on the starboard side may assume either orientation (Triggle et al., 1989). The space-filling model of nifedipine, solved by energy minimization by the Discover module of Insight II with the *cis* conformation of the ester group on the port side is shown in Fig. 3A. In this conformation, nifedipine has an elongated shape, with the long axis passing through the port and starboard sides.

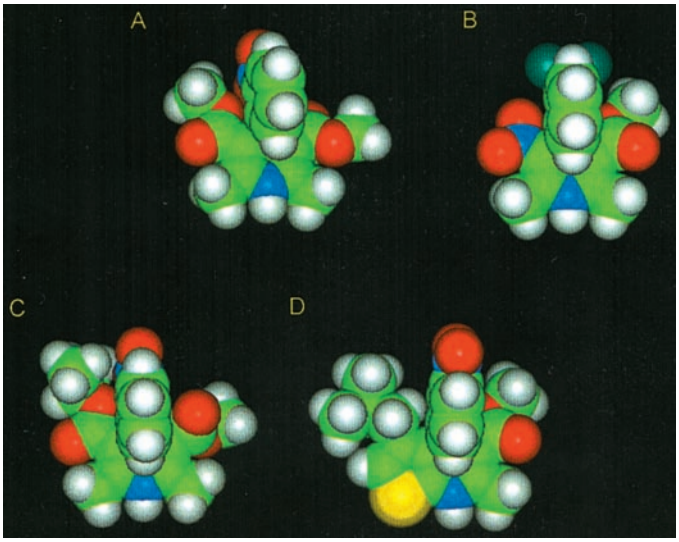

Fig. 3. Space-filled images of dihydropyridines. A, nifedipine. B, (−)-Bay K8644. C, derivative of nifedipine with an isopropyl ester group on the port side. D, DHP with fused thiophene ring.

The importance of a *cis* arrangement of the ester group on the port side for inhibitory biological activity of the DHP antagonists was shown by fused DHPs with an additional five-membered ring on the port side with the double bond, located exactly in the *cis* orientation relative to the double bond of the DHP ring (Goldmann and Stoltefuss, 1991). For example, the corresponding thiophene derivative of DHP (Adachi et al., 1988) (Fig. 4A) has shown a higher pharmacological activity than nifedipine itself. Its optimal space-filling image is shown in Fig. 3D. The high activity of DHP with the fused thiophene nucleus suggests that the ester group on the port side participates minimally in formation of hydrogen bonds with the DHP receptor site. The location of the lipophilic alkyl chain of the five-member thiophene ring is also important, because the derivative shown in Fig. 4B with the same alkyl substitution of the neighboring C-2 of the ring is practically inactive (Adachi et al., 1988).

The ester group on the port side plays a definitive role in the inhibitory function of DHP. A change in activity is mainly associated with an increase in the size of the aliphatic chain of the ester group on this side. The derivative of nifedipine with the isopropyl ester group in this position is more potent by a factor of 15 than regular nifedipine (Towart et al., 1981). Similar changes in the size of the ester group on the starboard side did not produce such a noticeable effect. The increase in activity with introduction of bulky nonpolar groups suggests that the ester group on the port side participates in hydrophobic interactions with the channel. Because of this, we begin with docking of the nifedipine derivative with the isopropyl ester group on the port side (Fig. 3C).

Agonist activity is produced only by substitutions by small polar groups in the ester group on the port side, enhancing the Ca^{2+} channel open probability. For example, the typical strong agonist (−)-Bay K8644 (shown in Fig. 3B as a space-filling image) has only a nitro group on the port side, whereas the enantiomer with the nitro group on the starboard side is still a Ca^{2+} antagonist (Goldmann and Stoltefuss, 1991). Therefore, comparison of the structures of the agonists with the antagonists allows us to conclude that introduction of the negative electrostatic field on the port side is important for

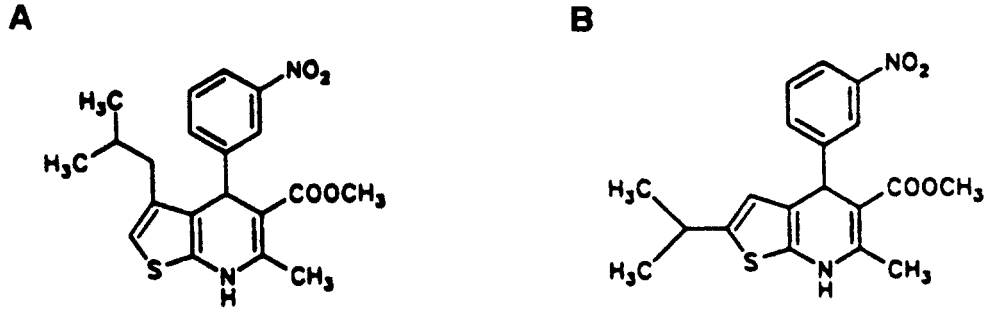

Fig. 4. Chemical structure of dihydropyridines with the port side fused thiophene rings. A, active derivative. B, nonactive derivative (Adachi et al., 1988).

agonist activity, whereas antagonist activity is connected intimately with the presence of the hydrophobic aliphatic chains inside the ester group on the port side of the DHP ring.

Evidence that agonists and antagonists bind to the same site includes similar effect of mutations in IIIS6 and IVS6 on affinities of the antagonist isradipine and the agonist (−)-Bay K8644 (Peterson et al., 1996). Specifically, both Tyr-1048 of IIIS6 and Tyr-1365 of IVS6 of the α_{1S} channel (corresponding to Tyr-1152 and Tyr-1463 of α_{1C}) are required for high-affinity binding of both the DHP antagonists and agonists (Peterson et al., 1996; Schuster et al., 1996). Therefore, we expect to dock (−)-Bay K8644 into the same III/IV crevice as nifedipine. However, this plan has an additional implication stated by Hockerman et al. (1997b): "If DHP is bound to a single site at which agonists increase Ca^{2+} current and agonists reduce Ca^{2+} current, then they cannot bind in a manner that blocks the pore".

Docking the Heterocyclic DHP Ring in the Interdomain III/IV Cleft. The interface crevice between domains III and IV, which we propose as a candidate for the binding site of DHP (Fig. 2, left), is restricted by the side chains of Tyr-1152 (IIIS6) and Tyr-1463 (IVS6) on the top and by the bulky nonpolar side chains of Ile-1163 and Ile-1471 on the bottom. The side chains of Phe-1159 (IIIS6) and Ala-1467 (IVS6) form the walls of the narrow cavity, with side-to-side separation that corresponds approximately to the width of an aromatic ring. In the DHP structure, the two aromatic ring choices are the heterocyclic DHP ring or the 4-aryl ring. However, if the 4-aryl substituent approaches the interface crevice, the long axis of the DHP ring adopts a perpendicular location relative to the pore axis, such that the ester groups on both sides contact the inner pore walls and do not allow the 4-aryl ring to move deeply into the cavity. In contrast, the DHP ring can be readily accommodated deep inside the cavity parallel to the pore axis, with its stern N-H group located close to the IIIS5 helix. In this case, the plane of the heterocyclic ring and its long port-starboard side axis is approximately parallel to the pore axis, whereas the 4-aryl ring is located perpendicular and closer to the center of the pore. The height of the proposed binding cavity corresponds to the size of the DHP ring along its long axis.

Two alternative orientations of the DHP ring are possible: starboard-side up/port-side down or the converse. Upon docking the nifedipine derivative with the port side isopropyl group (Fig. 3C), we find that the total energies of nonbonded interactions with the binding cavity are almost identical for the two orientations. The most obvious difference between the two orientations of the DHP ring is that in the first one the nonpolar part of the ester group on the port side (isopropyl) approaches the hydrophobic S6 crossing, approximately on the level of the side chains of Ile-1163 (IIIS6) and Ile-1471 (IVS6). However, both orientations produce effective contacts with the two DHP-sensitive Tyr-1152 and Tyr-1463 residues

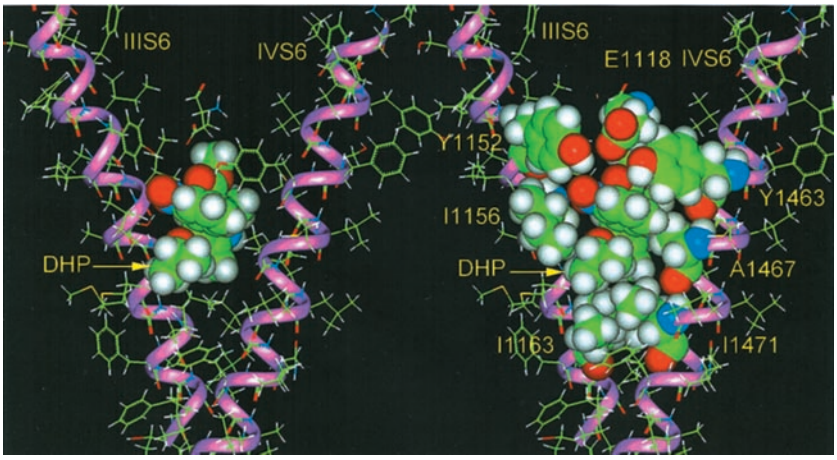

Fig. 5. DHP in the interface binding crevice. Optimal arrangement of DHP (the nifedipine derivative with isopropyl ester group on the port side) inside of the interface binding site between S6 α-helices of domains III and IV of the L-type Ca^{2+} channel (left). The ester group on the port side is located in the down orientation and adopts a *cis*-conformation relative to the DHP ring. Amino acid residues surrounding DHP are shown by space-filled images in the right. The 4-aryl ring interacts with the side chains of Tyr-1152 and Tyr-1463, whereas the nonpolar isopropyl group interacts with the hydrophobic side chains of Ile-1156, Ile-1163, and Ile-1471 on the bottom. The DHP ring is located in the depth of the crevice between the side chains of Phe-1159 and Ala-1467, parallel to the pore axis.

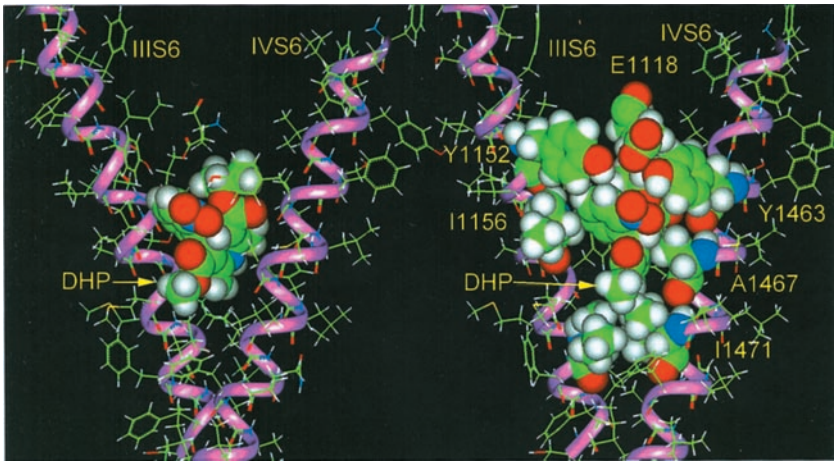

Fig. 6. Alternative orientation of DHP in the binding crevice. Optimal arrangement of the isopropyl derivative of nifedipine with the port side ester in the upward orientation.

(Figs. 5 and 6). Consequently, we docked the DHP ring in both conformations and determined interaction energies for comparison.

Arrangement of the nifedipine derivative with the additional isopropyl group on the port side located down was optimized (Fig. 5), allowing the side chains of residues of IIIS6 and IVS6 to reorient without movement of the main chains. The overall energy of nonbonded interactions with the binding cavity for this conformation was −35 kcal/mol. The aromatic ring of the 4-aryl substituent was located between the side chains of Tyr-1152 (IIIS6) and Tyr-1463 (IVS6), such that the nitro group in the ortho position could interact directly with the hydroxyl group of the side chain of Tyr-1152, whereas the aromatic ring itself could participate in a perpendicular aromatic-aromatic ring interaction with Tyr-1463 (Burley and Petsko, 1988). This proposed interaction of the 4-aryl ring with the side chain of Tyr-1152 meets the requirement for sensitivity of DHP binding not only to its substitution by Ala, but also the effect of substitution of this Tyr by Phe (Table 1) (Peterson et al., 1997). Tyr-1463 is also important for binding of isradipine (Table 1). The calculated energy of noncovalent interaction between DHP and the side chain of Tyr-1463 was −4.5 kcal/mol.

In this port-side-down orientation, the DHP ring itself is parallel to the side chain of Phe-1159 (IIIS6) with the interaction energy of about −4 kcal/mol, and it is located very close to Ala-1467 (IVS6), permitting the N-H group on the stern of the DHP ring to interact with π-electron cloud of the Phe-1159 aromatic ring. However, with this proposed orientation, neither N-H nor the carbonyl groups of the ester groups form direct hydrogen bonds. The ester group on the starboard side is located behind the side chains of Tyr-1152 and Tyr-1163 and near the side chain of Met-1464 (IVS6). Substitutions of Met-1464 also reduced affinity of DHP modestly (Hockerman et al., 1995). The starboard ester group also interacts with the side chain of Ile-1155 with calculated energy of −2.7 kcal/mol, but substitution with Ala failed to change the calculated interaction energy. This is an interesting example when mutation with alanine (Peterson et al., 1997) apparently fails to disrupt a real interaction.

The most notable distinction of this docking is the numerous nonpolar contacts of the port side ester group with hydrophobic residues on the bottom of the cavity. The isopropyl group of this derivative of nidefipine interacts not only with the side chains of Ile-1163 and Ile-1471, but also with the side chain of Ile-1156 (Fig. 5); experimentally, the Ala substitution of Ile-1156 produced the most remarkable decrease in isradipine affinity by 17-fold (Table 1; Peterson et al., 1997). Such an interaction is possible only in the *cis*-orientation of the port-side ester group. The energies of nonbonded interactions of the isopropyl group with each of the three Ile residues is at least −2.5 kcal/mol. The dominant role of nonpolar hydrophobic interactions for DHP is in accordance with the early suggestion that the DHP receptor site is hydrophobic, on the basis of the lipophilic character of the molecules (Herbette et al., 1989). It is not always possible to compare quantitatively the calculated energy of interaction with affinity change upon replacement with alanine, because interactions depend strongly on exact spacing and other factors that may not be modeled. The important conclusion is that the hydrophobic amino acid residues are located near critical components of the DHP ring.

The port-side-up orientation also produced optimal binding (Fig. 6), with overall energy of interaction of −33 kcal/mol, almost the same as for port-side down. The loss of nonbonded interactions of the isopropyl ester group with Ile-1156 and the S6 crossing residues of Ile-1163 and Ile-1471 is compensated by strong interactions of DHP with both Tyr-1152 and Phe-1159 (about −8 kcal/mol each). The absence of specific interactions with nonpolar residues of the S6 crossing (see later) is a disadvantage for this docking arrangement because hydrophobic interactions with the port side ester are important for DHP activity (Towart et al., 1981; Goldmann and Stoltefuss, 1991). The port-side-up orientation also seems to overestimate interactions with the side chains of Tyr-1152 and Phe-1159, because the experimental effects of substitution of these aromatic residues are modest (Table 1). Finally, this orientation is probably excluded by the docking interactions of agonists (see later). Therefore, pending more specific experimental evidence, we proceed with analysis of the port-side-down conformation for binding of DHP.

The proposed DHP binding site can also accommodate the DPH derivative with a fused thiophene ring on the port side (Fig. 4) only if the iso-C_4H_9 substituent of the thiophene ring is located in its 3rd position (Fig. 7, left). The height of the proposed binding cavity between Glu-1118 of the selectivity filter on the top and residues of the S6 crossing (Ile-1163 and Ile-1471) on the bottom corresponds exactly to the size of this derivative, which established the same optimal interactions with the cavity side chains as described for the nifedipine

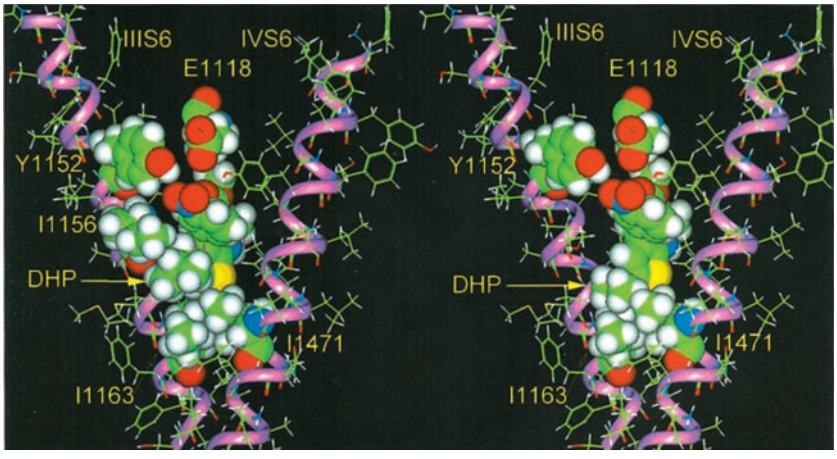

Fig. 7. DHPs with thiophene ring in the binding site. Arrangement inside the binding cavity of DHPs with fused thiophene rings (see Fig. 4), having the alkyl isobutyl substitution in the third position (active derivative) on the left, and in the second position (nonactive derivative) on the right. Substitution in the third position allows the optimal arrangement, whereas substitution in the second position leads to prohibited van der Waals contacts of the isobutyl group with bulky side chains on the bottom of the binding cavity.

derivative with the down orientation of the isopropyl ester group (Fig. 5). However, transfer of the iso-C_4H_9 group to the 2nd position (Fig. 7, right) resulted in formation of prohibited van der Waals contacts of this group with the bulky hydrophobic Ile-1163 and Ile-1471 on the bottom, which could explain the loss of biological activity by that molecule (Fig. 4B) (Adachi et al., 1988). The *trans* orientation of the aliphatic substituent of the ester group on the port side stereochemically coincides with location of the iso-C_4H_9 group substituting in the 2nd position of the thiophene ring (Fig. 7), again explaining the preference of the *cis* orientation of the ester group for DHP binding.

Possible Mechanism of DHP Block. Figures 5 and 7 present side views of the location of the DHP antagonists in the interface crevice between S6 helices of domains III and IV. The top view of the complex with the four domain assembly (Fig. 8) (Lipkind and Fozzard, 2001) demonstrates more clearly the location of the derivative of nifedipine (shown in violet) outside of the central pore and the Ca^{2+} permeation pathway. If the DHP do not obstruct the pore, then how do they block the current? The "teepee" arrangement of M2 in the KcsA channel structure as a model for the S6 α-helices of the Ca^{2+} channel provides a separation of the helix N-terminal ends, such that the side chains of one helix do not interact with each other; near the C-terminal ends, there is a densely packed bundle of the four α-helices (Doyle et al., 1998). In the Ca^{2+} channel model, the first level at which the S6 α-helices interact with each other is at residues corresponding to residues 104 and 107 of KcsA, so that the S6 immediate contacts are between the side chains of Val and Leu of domains I and II, Phe and Met of domains II and III, Ile and Ile of domains III and IV, and Phe and Leu of domains IV and I (Table 3). Voltage-activated channels seem to open by movement of the inner parts of the S6 α-helices (Liu et al., 1997). Electron paramagnetic resonance measurements of spin-labeled residues in KcsA suggested that opening involves a change in the diameter of the inner pore at the C-terminal crossing of the S6 helices (Perozo et al., 1998). In this proposed model of DHP binding in the Ca^{2+} channel, the nonpolar alkyl substituents of the port side ester interact with hydrophobic residues at the bottom of the binding cavity that forms the crossing between IIIS6 and IVS6 helices (Fig. 5). The DHP antagonists bind with higher affinity to the inactivated (closed) state of the channel (Hockerman et al., 1997b). Both observations suggest that the hydrophobic interactions of the port-side ester group of the DHP antagonists with the hydrophobic residues could stabilize a closed state of the L-type Ca^{2+} channel by preventing conformational changes at the S6 crossing that are required for gating.

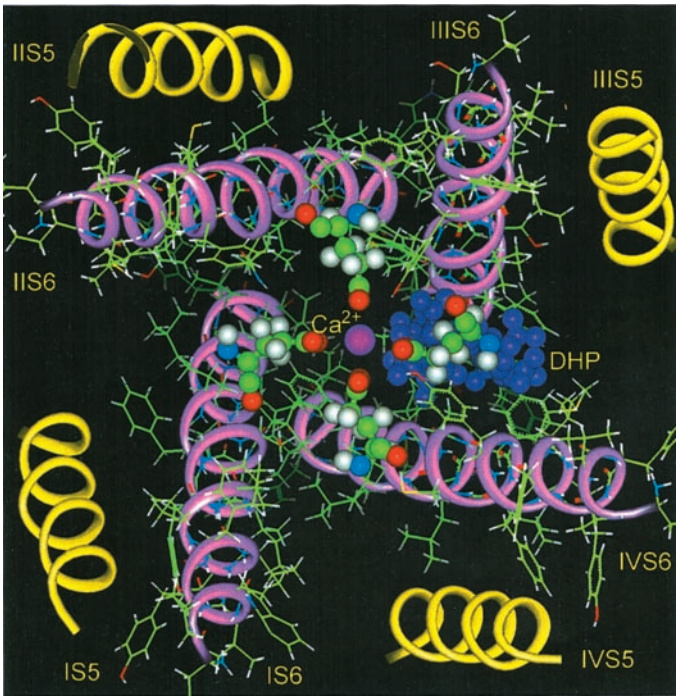

Fig. 8. Location of DHP outside the central pore of the L-type Ca^{2+} channel. Top view of the four-domain organization of the Ca^{2+} channel with the DHP molecule (shown by violet balls and sticks) located in the interface between domains III and IV. The selectivity filter glutamates and a Ca^{2+} ion (pink ball) are also distinguished.

DHP Agonist Binding Site. Docking of the agonist (−)-Bay K8644 (Fig. 3B) inside the proposed binding site was by superposition with nifedipine in its optimal arrangement, followed by minimization of the potential energy, as shown in Fig. 9. The DHP and 4-aryl rings of the agonist established the same optimal energetic interactions with the side chains of Tyr-1152 and Tyr-1463 and of the other residues of the crevice/pore as they did for binding of antagonists (Fig. 5). With the port-side-down orientation, the specific nitro group on the port side of the DHP ring of the agonist (Fig. 3B) is directed into the pore. In this orientation the NO_2 does not participate in specific interactions with the IIIS6/IVS6 inter-

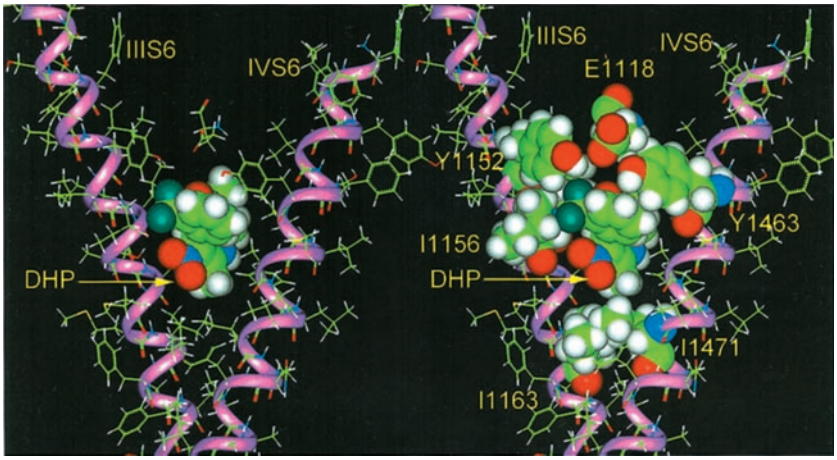

Fig. 9. Binding of (−)-Bay K8644. Model of binding of the derivative with agonist activity inside the interface III/IV domains of the Ca^{2+} channel with the nitro group on the port side of the DHP ring facing the pore.

face. Indeed, its substitution by hydrogen maintains the polarization and still results in agonist behavior (Goldmann and Stoltefuss, 1991). With the port side up, this nitro group would be screened from the pore by side chains of Tyr-1152, Tyr-1463, Glu-1118, and other residues of the IIIS6 and IVS6 helices, which could lead to a loss of agonist activity. The proposed arrangement of (−)-Bay K8644 also allowed optimal docking of another agonist CGP 28-392, which includes the five-membered lactone ring on the port side (Goldmann and Stoltefuss, 1991). Both of its oxygens coincided with the NO_2 group of the DHP ring of (−)-Bay K8644. However, in the case of docking of (+)-Bay K8644 in the starboard-side-down orientation, the location of the NO_2 group of the DHP ring coincided with location of the similar NO_2 group of (−)-Bay K8644. Then (+)-Bay K8644 could act as an agonist. However, it is an antagonist, excluding the starboard-down orientation of DHPs inside the receptor site. With orientation of the port side of (−)-Bay K8644 down, the NO_2 group faces the pore, near to the S6 crossing. The loss of hydrophobic interactions with the S6 crossing residues, which are so important for binding of antagonists, suggests why there is low affinity of the agonist for the inactivated state, and in turn, why it may destabilize the inactivated state and increase the probability of channel opening (Hockerman et al., 1997b). In the proposed arrangement of antagonists, the electronic π-cloud of the aromatic 4-aryl ring is screened by the aliphatic chain on the port side ester group. However, with agonist binding, the π-cloud of the 4-aryl ring and the port side NO_2 group produce additional negative electrostatic potential inside the pore that might also contribute to stimulation of Ca^{2+} permeation (Goldmann and Stoltefuss, 1991).

DHPs and the Selectivity Filter. Direct interactions between the DHP molecule and the selectivity filter, its glutamic acids, and Ca^{2+} ions in the selectivity filter were not considered during the development of the binding pocket, because mutation of the selectivity filter glutamates only moderately reduce the affinity of isradipine binding (by ~4-fold; Peterson and Catterall, 1995). The high-affinity binding of Ca^{2+} in the pore also stimulates binding of DHPs (Peterson and Catterall, 1995; Mitterdorfer et al., 1995). It seems unlikely that Ca^{2+} directly interacts with the lipophilic DHP. Indeed, the presence of such strong acceptors of Ca^{2+} as four glutamates should preclude direct interactions with the neutral DHPs by a competitive mechanism. Peterson and Catterall (1995) and Hockerman et al. (1997a) consider a possible allosteric mechanism of interaction between Ca^{2+} and the DHP binding site. It is entirely possible that the presence of Ca^{2+} in the selectivity filter also influences the conformational state of the binding site immediately below the domain III glutamic acid.

Next, we considered arrangement of DHPs on the III/IV interface, outside of the pore and the selectivity filter. The fact that BTZs, located on the same level of the pore as DHPs (Hering et al., 1996), do not inhibit but instead stimulate binding of DHPs supports this proposal. Location of bound DHPs outside the pore is also compatible with new data on block of L-type Ca^{2+} channels by DHPs where the DHP moiety is attached to a charged head group through short alkyl spacers. J. Xia and R. Kass (personal communication) have shown: 1) No effect of test voltage on block by the DHP with a tethered charge, presumably because the charged head group fails to enter the electric field; and 2) DHPs display similar potency when the charged head group was positive or negative, which excludes their interaction with the selectivity filter. These results indicate that DHPs reach their binding site below the selectivity filter without passing through the filter itself. Although our model does not show this alternative path, it does locate the binding in a space between IIIS5, IIIS6, and IVS6, immediately below the domain III P loop α-helix, suggesting that a lipophilic path for the DHP molecules may exist behind the P loop. This conclusion is in agreement with the recent observation that mutation of Phe-1112 (F1112A) of the P loop of domain III of α_{1C}, which we located inside of the hydrophobic α-helical segment of this P loop (Lipkind and Fozzard, 2001), also modulated binding of both agonist and antagonist DHPs (Yamaguchi and Adachi-Akahane, 2002). In addition, Yamaguchi et al. (2000) report that the alanine mutation of Ser-1115 in the IIIP, which we locate at the top of the binding cleft, markedly reduced agonist efficacy. Therefore, the N-terminal segment of IIIP also could play an important functional role, allowing DHPs to reach the interface binding site inside the L-type Ca^{2+} channel.

Docking of PAA Inside the Ca^{2+} Channel Pore. PAAs block L-type Ca^{2+} channels from the intracellular side and are considered to block by occlusion of the central permeation path (Hockerman et al., 1997b). Three molecules within the PAA class have been extensively studied: verapamil (shown in Fig. 10 by a space-filled image), D888, and methoxyverapamil. D888 contains only one *meta*-methoxy group inside of the aromatic ring of the phenylethyl part, whereas verapamil contains two methoxy groups in *meta*- and *para*- positions. D888 blocks the channel with higher affinity than verapamil (about 300-fold) (Johnson et al., 1996), although verapamil is the only drug in this class currently in clinical use. The levorotatory (−)-enantiomers of PAAs are more potent than the dextrorotatory (+)-enantiomers (Ferry et al., 1984). Here, the (−)-isomers of verapamil and its derivatives are considered, with clockwise arrangement of aryl, isopropyl, and

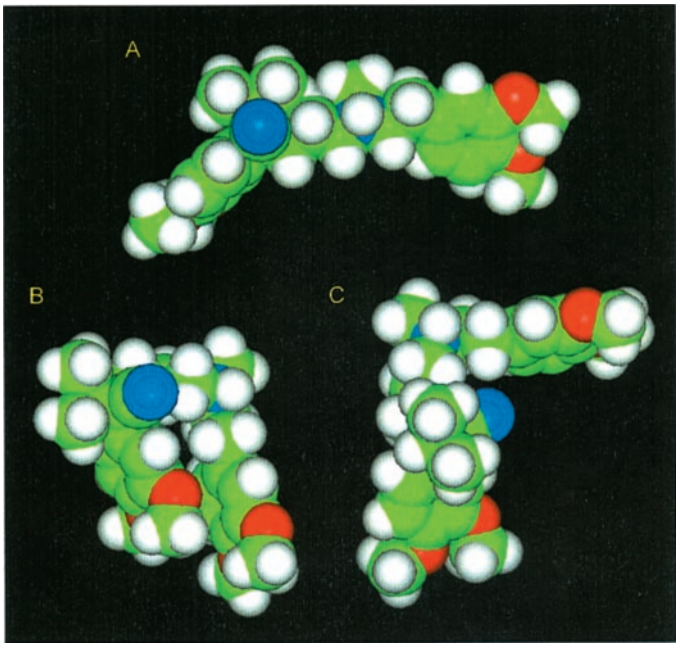

Fig. 10. Verapamil conformations. Verapamil is shown in space-filling images in the extended (A), folded (B), and half-folded (C) conformations.

C≡N groups around the chiral center upward and the rest of the structure downward (Carey, 1996).

Verapamil can adopt three structural forms (or conformational shapes): extended, folded, and half-folded. The energetically optimal conformations of each shape are shown in Fig. 10. The folded conformation is stabilized by nonbonded interactions of dimethoxyaryl rings on the opposite ends of verapamil, and this should be the most stable conformation of the isolated drug. The conformation of the drug during its interaction with the channel is uncertain, making it less useful in developing a model of the binding site. However, because PAAs both block the pore and inhibit binding of DHP, we propose that during its formation of a complex with the channel, the PAA drug adopts the half-folded shape, allowing it to occlude the interface III/IV crevice and simultaneously occupy the central pore.

The proposed docking of D888 in its half-folded conformation is shown in Fig. 11. D888 predominately interacts with transmembrane segment IVS6 (Hockerman et al., 1997b), and makes immediate van der Waals contacts with the side chains of three amino acid residues, Tyr-1463, Ala-1467, and Ile-1470, which have been shown to be the most critical residues for PAA binding (Hockerman et al., 1995). The aromatic ring of the phenylethylamine part of this derivative is located inside the interface III/IV crevice, where we have also proposed that the DHP ring binds, thereby participating in aromatic-aromatic interaction with Tyr-1463 (Fig. 11) with an energy of nonbonded interaction of about −5 kcal/mol. This permits the isopropyl substituent of the alkyl chain of D888 to be located between the side chains of Ala-1467 and Ile-1470, whereas the methyl groups of both methoxy groups, substituting for the second phenyl ring on the opposite side, can reach and surround Ile-1470, and this phenyl ring is located inside the pore. These contacts between D888 and IVS6 generate the hydrophobic component of the potential energy of interaction between the molecules. In this arrangement, the presence of the second *para*-methoxy group in the aromatic ring of phenylethylamine introduces interference with the side chains of residues in the back wall of the interface crevice (Met-1464), which might lead to the reduced binding affinity of verapamil relative to D888.

The recent experimental finding that a mutation in the IIIS5 α-helix (T1039Y) has improved binding of devapamil (Huber et al., 2002) supports the requirement that one of the aromatic rings of PAA in the bound state occupies the III/IV interface crevice. Such modulation of binding is possible if PAAs also occlude the space outside of the central pore that is close to the back wall of our proposed DHP binding cavity.

In contrast to the DHP molecules, the PAA molecules are predominantly positively charged at physiological pH because of the tertiary amine, and therefore they could interact electrostatically with the only negative charges in the central pore - the selectivity filter glutamates. In the half-folded conformation that we have chosen for docking (Fig. 11), the central amine is on the corner between two perpendicular fragments of the PAA molecule. With the aromatic ring of phenylethylamine inside the DHP binding pocket, this amine is directed very close to the carboxylate group of the side chain of Glu-1118 (domain III) and also to that of Glu-1419 (domain IV) (Fig. 11), with formation of corresponding ion pairs. Experimentally, substitution of Glu-1118 and Glu-1419 by glutamines resulted in a reduction in D888 affinity by 20- and 15-fold, respectively (Hockerman et al., 1997a). In terms of free energies, such changes correspond to about −1.5 kcal/mol. The same mutations produce only a 4-fold change in the affinity of DHP (Peterson and Catterall, 1995). In the proposed orientation of D888, its amine could also interact with the side chain of Tyr-1463 (IVS6) and possibly with its hydroxyl (Fig. 11). According to mutational data, the mutant Y1463F substantially disrupted block by D888 (Johnson et al., 1996), which Hockerman et al. (1997a) suggested was the result of a hydrogen bond between Tyr-1463 and D888. If the amine is very close to Tyr-1463, then its methyl substituent is directed to the side chain of Tyr-1152 (IIIS6), so Tyr-1152 would not be important for PAA binding. Correspondingly, its replacement with Ala did not decrease the affinity for D888 (Table 2). Therefore, in this proposed model, PAA binding involves simultaneous hydrophobic and ionic interactions with the selectivity filter, the interdomain III/IV crevice, and the pore of the L-type Ca^{2+} channel.

General Model Features. Spacial organization of the S5 and S6 transmembrane α-helices of the Ca^{2+} channel on the basis of the M1 and M2 segments of KcsA is plausible and has been used by several investigators (Huber et al., 2000; Lipkind and Fozzard, 2001; Zhorov et al., 2001). However, careful alignment of the α-helices is critical if the residues facing the pore and the adjacent S6 segments are to include the residues experimentally shown to be required for drug interaction. The KcsA P loop is inappropriate for the Ca^{2+} channel

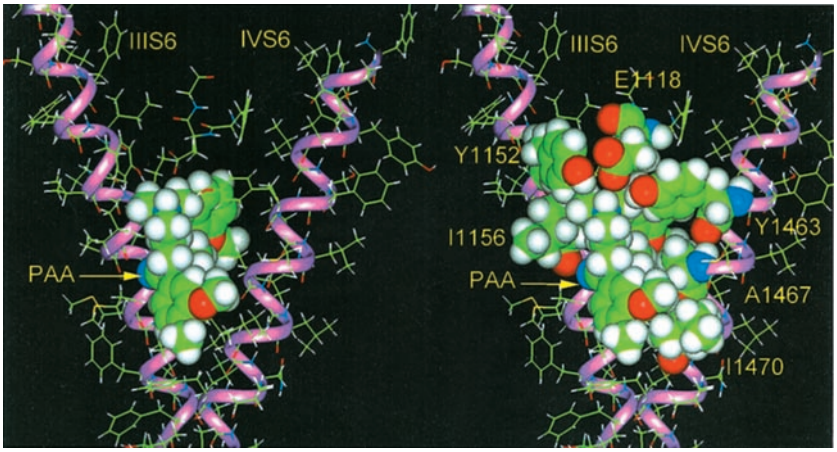

Fig. 11. Binding of D888. Binding of desmethoxyverapamil (D888) in the half-folded conformation inside of the pore and the interface crevice between domains III and IV. The aromatic rings on the ends of D888 interact with the side chains of Tyr-1463 and Ile-1470, correspondingly. The central amine interacts directly with the carboxylate of the side chain of Glu-1118 of the selectivity filter, thereby blocking permeation.

because of the need for direct involvement of the side chains of the glutamate residues of the selectivity filter in Ca^{2+} binding. In addition, the KcsA P loops would cover most of the critical S6 residues involved in the drug interaction. The exact location of the selectivity filter is critical, because it represents an upper spacial limit for the drug binding site and because drug affinities are influenced by ions in the selectivity filter.

The KcsA channel coordinates probably correspond to a closed conformation of the channel (Jiang et al., 2002b), so it is likely that our modeled Ca^{2+} channel pore is also closed. Little is known about the conformational changes that occur during voltage-dependent L-type Ca^{2+} channel activation and inactivation gating. Mutational studies suggest that the S4 segments from only domains I and III are involved in activation (Garcia et al., 1997), and multiple regions seem to play a role in some type of inactivation (Hering et al., 2000). A K^+ channel with a homologous two-transmembrane segment subunit structure (MthK), which is open in the presence of low concentrations of Ca^{2+}, has now been structurally determined by X-ray crystallography and it is almost identical to that of KcsA (Jiang et al., 2002a). However, the conformation of its M2 helices (analogous to the S6 helices of the Shaker channel) is different from that of the KcsA channel, corresponding to an open state. In the MthK structure, the lower half of the M2 helix is bent outward, as the result of a flexible hinge formed by a highly conserved glycine residue (Gly-83 in MthK or Gly-99 in KcsA), thereby avoiding the helical crossover seen in the KcsA channel and resulting in opening of the pore vestibule to a diameter of 12 Å. At first glance, this seems to offer us the opportunity to model the L-type Ca^{2+} channel in its activated-open conformation, allowing us to compare changes of drug interaction with gating. However, there is no structural equivalent to the MthK hinge in the domains IIIS6 and IVS6 α-helices because these Ca^{2+} channel domains contain neither this glycine residue nor helix-breaking prolines; instead, conformationally restricted isoleucine or cysteine residues are present in the corresponding positions (Table 3). Consequently,. The S6 segments of domains I and II do contain the important glycine residue, which is conserved in all isoforms of the Ca^{2+} channel (see Stea et al., 1994, and our alignment for IS6 and IIS6 in Lipkind and Fozzard, 2001). It is likely that gating of the Ca^{2+} channel is different, with hinged motion of domains I and II S6 α-helices, whereas those of domains III and IV remain predominantly straight. This supports our use of the KcsA structure in modeling the core structure of domains III and IV for the drug high-affinity state.

Although it is tempting to suggest that the modeled conformation with crossover of the domains III and IV helices is close to the structure of the normal inactivated state, drug interaction could induce a different closed state. Berjukow et al. (2000) showed that alanine substitution for the residues corresponding to Ile-1470 and Ile-1471 at the crossover slowed the onset of inactivation. In addition, substitution of some of the hydrophobic residues closer to the C-end of IIIS6 can dramatically decrease the rate of inactivation (IF1612/1613AA in IIIS6 of $Ca_v2.1$; Hering et al., 2000; Sokolov et al., 2000). Both observations are consistent with our proposal that DHP antagonists could interact with a closed state that resembles the inactivated state and stabilize it by interaction at the level of the IIIS6 and IVS6 helical crossover. If, as predicted by the model, DHP antagonists bind to Ile-1163 and Ile-1471 with a total of −5 kcal/mol, and this interaction occurs only in the inactivated state, then this interaction could account for the difference in affinity between the hyperpolarized, resting state and a depolarized state. We hypothesize that the different affinities of the gating states can be mediated by relatively small conformational changes inside the IIIS6/IVS6 binding site, sufficient to disrupt short-range hydrophobic interactions.

Because of the similarity of DHP antagonist and agonist binding interaction, we endorse the strong argument that DHP must not block the pore (Hockerman et al., 1997b), whereas the PAA site must overlap and simultaneously block the pore. This requires that DHP influence the current by altering gating, which is more easily satisfied if the drug binds close to the gating apparatus. We have suggested that this gating effect might be mediated via interaction with the side chains of hydrophobic residues at the S6 helix crossing point, because this is the location in the binding site at which the critical difference between antagonist and agonist DHP binding is found and at which mutations produce changes in inactivation behavior of the L-type Ca^{2+} channel, as well as in the similar Na^+ channel (McPhee et al., 1995; Sunami et al., 2000). The interactions suggested by this model are amenable to test by mutant cycle analysis between mutated channel residues and analogs of the drugs, similar to studies of the binding interactions for guanidinium toxins and μ-conotoxin in the vestibule of Na^+ channels (Chang et al., 1998; Dudley et al., 2000; Penzotti et al., 2001).

Conclusions

To test the domain interface hypothesis for the formation of a binding site for DHP and PAA drugs, we aligned the sequences of the domain III S5 and S6 and domain IV S6 of the L-type Ca^{2+} channel, using the spacial orientation of the backbones of M1 and M2 α-helices of the KcsA channel derived from its X-ray crystal structure, maximizing the coincidence of residues known to affect the drug biological activity with the pore-facing residues of KcsA. The resulting structure formed a crevice between domain III S6 and domain IV S6, with its top formed by the domain III P loop and its back formed partly by domain III S5. DHPs were considered in their preferred *cis*- conformation of the port side ester group. For the optimal arrangement of a derivative of nifedipine, the 4-aryl ring interacted with the side chains of Tyr-1152 and Tyr-1463, the DHP ring itself was located parallel to the axis of the pore in the crevice depth, and the nonpolar isopropyl substituent of the ester group on the port side participated in strong interactions with the side chains of Ile-1156, Ile-1163, and Ile-1471 on the bottom. The model allowed an explanation of the different inhibitory activity of DHPs with fused thiophene rings on the port side with alkyl substitutions in the 3rd position (active) and in the 2nd position (inactive). DHP agonists adopted a similar arrangement inside the interface crevice, so that both agonists and antagonists were located outside the central pore, where they do not block by pore occlusion. However, the antagonists had nonpolar interactions with residues at the crossing of domains III and IV S6 helices at the bottom of the crevice that could prevent helical movements involved in activation by stabilizing the closed state; agonists in this conformation

were not able to interact with the hydrophobic crossing residues, destabilizing the closed state. PAAs were docked in their half-folded conformation with the aromatic ring of the phenylethylamine part of D888 located in the interface III/IV crevice in proximity to the side chain of Tyr-1463 of IV S6, thereby blocking binding of DHP molecules. The second aromatic ring in the pore interacted with the side chain of Ile-1470. The central amine of D888 interacted directly by a salt bridge with the carboxylate side chain of Glu-1118 of the selectivity filter, blocking Ca^{2+} permeation.

Acknowledgments

We thank Dr. Dorothy Hanck for advice during the course of development of this model.

References

Adachi I, Yamamori T, Hiramatsu Y, Sakai K, Mihara S, Kawakami M, Masui M, Uno O, and Ueda M (1988) Studies of dihydropyridines. III. Synthesis of 4,7-dihydrothieno [2,3-*b*]-pyridines with vasodilator and antihypertensive activities. *Chem Pharm Bull* **36:**4389–4402.

Bangalore R, Baindur N, Rutledge A, Triggle D, and Kass RS (1994) L-type Ca^{2+} channels: asymmetrical intramembrane binding domain revealed by variable length, permanently charged 1,4-dihydropyridines. *Mol Pharmacol* **46:**660–666.

Berjukow S, Marksteiner R, Gapp F, Sinnegger MJ, and Hering S (2000) Molecular mechanism of calcium channel block by isradipine. *J Biol Chem* **275:**22114–22120.

Burley SK and Petsko GA (1988) Weakly polar interactions in proteins. *Adv Protein Chem* **39:**125–189.

Carey FA (1996) *Organic Chemistry*, 3rd ed., McGraw-Hill, NY.

Chang NS, French RJ, Lipkind GM, Fozzard HA, and Dudley SC Jr (1998) Predominant interactions between μ-conotoxin Arg-13 and the skeletal muscle Na^+ channel localized by mutant cycle analysis. *Biochemistry* **37:**4407–4419.

Doyle DA, Cabral JM, Pfuetzner RA, Kuo A, Gulbis JM, Cohen SL, Chait BT, and MacKinnon R (1998) The structure of the potassium channel: molecular basis of K^+ conduction and selectivity. *Science (Wash DC)* **280:**69–74.

Dudley SC Jr, Chang NS. Hall J, Lipkind GM, Fozzard HA and French RJ (2000) μ-Conotoxin GIIIA interactions with the voltage-gated Na^+ channel predict a clockwise arrangement of the domains. *J Gen Physiol* **116:**679–689.

Ferry DR, Goll A, Gadow C, and Glossmann H (1984) (−)-^{3}H-Desmethoxyverapamil labeling of putative calcium channels in brain: autoradiographic distribution and allosteric coupling to 1,4-dihydropyridine and diltiazem binding sites. *Naunyn-Schmiedeberg's Arch Pharmacol* **327:**183–187.

Garcia J, Nakai J, Imoto K, and Beam KG (1997) Role of S4 segments and the leucine heptad motif in the activation of an L-type calcium channel. *Biophys J* **72:**2515–2523.

Goldmann S and Stoltefuss J (1991) 1,4-dihydropyridines: effects of chirality and conformation on the calcium antagonist and calcium agonist activities. *Angew Chem Int Ed Engl* **30:**1559–1578.

Grabner M, Wang Z, Hering S, Striessnig J, and Glossmann H (1996) Transfer of 1,4-dihydropyridine sensitivity from L-type to class A(B1) calcium channels. *Neuron* **16:**207–218.

He M, Bodi I, Mikala G, and Schwartz A (1997) Motif IIIS5 of L-type calcium channels involved in the dihydropyridine binding site. *J Biol Chem* **271:**2629–2633.

Heinemann SM, Terlau H, Stühmer W, Imoto K, and Numa S (1992) Calcium channel characteristics conferred on the sodium channel by single mutations. *Nature (Lond)* **356:**441–443.

Herbette LG, Vant-Erve VM, and Rhodes DG (1989) Interaction of 1,4-dihydropyridine calcium channel antagonists with biological membranes: lipid bilayer partitioning could occur before drug binding to receptors. *J Mol Cell Cardiol* **21:**187–201.

Hering S, Berjukow S, Sokolov S, Marksteiner R, Weiss RG, Kraus R, and Timin EN (2000) Molecular determinants of inactivation in voltage-gated Ca^{2+} channels. *J Physiol* **528:**237–249.

Hering S, Aczel S, Grabner M, Döring F, Berjukow S, Mitterdorfer J, Sinnegger MJ, Striessnig J, Degtiar VE, Wang Z, et al. (1996) Transfer of high sensitivity for benzothiazepines from L-type to class A(B1) calcium channels. *J Biol Chem* **271:**24471–24475.

Hille B (2001) *Ionic Channels of Excitable Membranes*, 3rd Ed, Sinauer, Sunderland, MA.

Hockerman GH, Johnson BD, Abbott MR, Scheuer T, and Catterall WA (1997a) Molecular determinants of high-affinity phenylalkylamine block of L-type calcium channels in transmembrane segment IIIS6 and the pore region of the α1 subunit. *J Biol Chem* **272:**18759–18765.

Hockerman GH, Johnson BD, Scheuer T, and Catterall WA (1995) Molecular determinants of high-affinity phenylalkylamine block of L-type calcium channels. *J Biol Chem* **270:**22119–22122.

Hockerman GH, Peterson BZ, Johnson BD, and Catterall WA (1997b) Molecular determinants of drug binding and action of L-type calcium channels. *Annu Rev Pharmacol Toxicol* **37:**361–396.

Huber I, Sinnegger J, Koschak A, and Striessnig J (2002) Phenylalkylamine interaction with transmembrane segment IIIS5 of L-type Ca^{2+} channel α_{1C} subunits (Abstract). *Biophys J* **82:**103a

Huber I, Wappl E, Herzog A, Mitterdorfer J, Glossmann H, Langer T, and Striessnig J (2000) Conserved Ca^{2+} antagonist-binding properties and putative folding structure of a recombinant high-affinity dihydropyridine binding domain. *Biochem J* **347:**829–836.

Jiang Y, Lee A, Chen J, Cadene M, Chait BT, and MacKinnon R (2002a) Crystal structure and mechanism of a calcium-gated potassium channel. *Nature (Lond)* **417:**515–522.

Jiang Y, Lee A, Chen J, Cadene M, Chait BT, and MacKinnon R (2002b) The open conformation of potassium channels. *Nature (Lond)* **417:**523–526.

Johnson BJ, Hockerman GH, Scheuer T, and Catterall WA (1996) Distinct effects of mutations in transmembrane segment IVS6 on block of L-type calcium channels by structurally similar phenylalkylamines. *Mol Pharmacol* **50:**1388–1400.

Lipkind GM and Fozzard HA (2000) KcsA crystal structure as framework for a molecular model of the Na^+ channel pore. *Biochemistry* **39:**8161–8170.

Lipkind GM and Fozzard HA (2001) Modeling of the outer vestibule and selectivity filter of the L-type Ca^{2+} channel. *Biochemistry* **40:**6786–6794.

Liu Y, Holmgren M, Jurman ME, and Yellen G (1997) Gated access to the pore of a voltage-dependent K^+ channel. *Neuron* **19:**175–184.

McPhee JC, Ragsdale DS, Scheuer T, and Catterall WA (1995) A critical role for transmembrane segment IVS6 of the sodium channel alpha subunit in fast inactivation. *J Biol Chem* **270:**12025–12034.

Mitterdorfer J, Grabner M, Kraus RL, Hering S, Prinz H, Glossmann H, and Striessnig J (1998) Molecular basis of drug interaction with L-type Ca^{2+} channels. *J Bioenerg Biomembr* **30:**319–334.

Mitterdorfer J, Sinnegger MJ, Grabner M, Striessnig J, and Glossmann H (1995) Coordination of Ca^{2+} by the pore region glutamates is essential for high-affinity dihydropyridine binding to the cardiac Ca^{2+} channel alpha 1 subunit. *Biochemistry* **34:**9350–9355.

Mitterdorfer J, Wang Z, Sinnegger MJ, Hering S, Striessnig J, Grabner M, and Glossmann H (1996) Two amino acid residues in the IIIS5 segment of L-type calcium channels differentially contribute to 1,4-dihydropyridine sensitivity. *J Biol Chem* **271:**30330–30335.

Penzotti JL, Lipkind GM, Fozzard HA, and Dudley SC Jr (2001) Specific neosaxitoxin interactions with the Na^+ channel outer vestibule determined by mutant cycle analysis. *Biophys J* **80:**698–706.

Perozo E, Cortes DM, and Cuello LG (1998) Three-dimensional architecture and gating mechanisms of a K^+ channel studied by EPR spectroscopy. *Nature (Lond) Struct Biol* **5:**459–469.

Peterson BZ and Catterall WA (1995) Calcium binding in the pore of L-type calcium channels modulates high-affinity dihydropyridine binding. *J Biol Chem* **270:**18201–18204.

Peterson BZ, Johnson BD, Hockerman GH, Acheson M, Scheuer T, and Catterall WA (1997) Analysis of the dihydropyridine receptor site of L-type calcium channels by alanine-scanning mutagenesis. *J Biol Chem* **272:**18752–18758.

Peterson BZ, Tanada TN, and Catterall WA (1996) Molecular determinants of high-affinity dihydropyridine binding in L-type calcium channels. *J Biol Chem* **271:**5293–5296.

Schuster A, Lacinova L, Klugbauer N, Ito H, Birnbaumer L, and Hofmann F (1996) The IVS6 segment of the L-type calcium channel is critical for the action of dihydropyridines and phenylalkylamines. *EMBO J* **15:**2365–2370.

Sokolov S, Weiss RG, Timin EN, and Hering S (2000) Modulation of slow inactivation in class A Ca^{2+} channels by β-subunits. *J Physiol* **527:**445–454.

Stea A, Soong TW, and Snutch TP (1994) Voltage-gated calcium channels, in *Handbook of Receptors and Channels* (North RA ed) Vol 2, pp 113–152, CRC Press, Boca Raton, FL.

Sunami A, Glaaser IW, Lipkind GM, and Fozzard HA (2000) Characterizing the structure and orientation of domain IVS6 of sodium channels. *Biophys J* **80:**231a.

Towart R, Wehinger E, and Meyer H (1981) Effects of unsymmetrical ester substituted 1,4-dihydropyridine derivatives and their optical isomers on contraction of smooth muscle. *Naunyn-Schmiedeberg's Arch Pharmacol* **317:**183–185.

Triggle DJ (1999) The pharmacology of ion channels: with particular reference to voltage-gated Ca^{2+} channels. *Eur J Biochem* **375:**311–325.

Triggle DJ, Langs DA, and Janis RA (1989) Ca^{2+} channel ligands: structure-function relationships of the 1,4-dihydropyridines. *Med Res Rev* **9:**123–180.

Wappl E, Mitterdorfer J, Glossmann H, and Striessnig J (2001) Mechanism of dihydropyridine interaction with critical binding residues of L-type Ca^{2+} channel α1 subunits. *J Biol Chem* **276:**12730–12735.

Yamaguchi S, Okamura Y, Nagao T, and Adachi-Akahane S (2000) Serine residue in the IIIS5–S6 linker of the L-type Ca^{2+} channel α_{1C} subunit is the critical determinant of the action of dihydropyridine Ca^{2+} channel agonists. *J Biol Chem* **275:**41504–41511.

Yamaguchi S and Adachi-Akahane S (2002) Role of the IIIS5–S6 linker of the L-type Ca^{2+} channel α_{1C} subunit in the action of Ca^{2+} channel agonist. *Biophys J* **82:**103a.

Yang J, Ellinor PT, Sather WA, Zhang JF, and Tsien RW (1993) Molecular determinants of Ca^{2+} selectivity and ion permeation in L-type Ca^{2+} channels. *Nature (Lond)* **366:**158–161.

Zhorov BS, Volkman EV, and Ananthanarayanan VS (2001) Homology model of dihydropyridine receptor: implications for L-type Ca^{2+} channel modulation by agonists and antagonists. *Arch Biochem Biophys* **393:**22–41.

Address correspondence to: Dr. Harry A. Fozzard, PO Box 574, 16 Georgianna Lane, Dana, NC 28724. E-mail: hafozzar@midway.uchicago.edu